

# COMPARING SEA LEVEL RESPONSE AT MONTEREY, CALIFORNIA FROM THE 1989 LOMA PRIETA EARTHQUAKE AND THE 1964 GREAT ALASKAN EARTHQUAKE

L. C. Breaker<sup>1</sup>, T.S. Murty<sup>2</sup>, Jerrold G. Norton<sup>3</sup>, & Dustin Carroll<sup>1</sup>

<sup>1</sup>Moss Landing Marine Laboratories, Moss Landing, California

<sup>2</sup>University of Ottawa, Ottawa, Canada

<sup>3</sup>Southwest Fisheries Science Center/NMFS/NOAA, La Jolla, California

Email: <mailto:Lbreaker@mlml.calstate.edu>

## ABSTRACT

Two of the largest earthquakes to affect water levels in Monterey Bay in recent years were the Loma Prieta Earthquake (LPE) of 1989 with a moment magnitude of 6.9, and the Great Alaskan Earthquake (GAE) of 1964 with a moment magnitude of 9.2. In this study, we compare the sea level response of these events with a primary focus on their frequency content and how the bay affected it, itself. Singular Spectrum Analysis (SSA) was employed to extract the primary frequencies associated with each event. It is not clear how or exactly where the tsunami associated with the LPE was generated, but it occurred inside the bay and most likely began to take on the characteristics of a seiche by the time it reached the tide gauge in Monterey Harbor. Results of the SSA decomposition revealed two primary periods of oscillation, 9-10 minutes, and 31-32 minutes. The first oscillation is in agreement with the range of periods for the expected natural oscillations of Monterey Harbor, and the second oscillation is consistent with a bay-wide oscillation or seiche mode. SSA decomposition of the GAE revealed several sequences of oscillations all with a period of approximately 37 minutes, which corresponds to the predicted, and previously observed, transverse mode of oscillation for Monterey Bay. In this case, it appears that this tsunami produced quarter-wave resonance within the bay consistent with its seiche-like response. Overall, the sea level responses to the LPE and GAE differed greatly, not only because of the large difference in their magnitudes but also because the driving force in one case occurred inside the bay (LPE), and in the second, outside the bay (GAE). As a result, different modes of oscillation were excited.

*Science of Tsunami Hazards, Vol. 28, No. 5, page 255 (2009)*

## 1. INTRODUCTION

In the past 50 years, two of the largest earthquakes to affect water levels in Monterey Bay were the Loma Prieta Earthquake of 1989 and the Great Alaskan Earthquake of 1964. The epicenter of the Loma Prieta Earthquake (LPE) occurred relatively close to Monterey Bay (Fig. 1) and the bay was part of the area affected by the event whereas the Great Alaskan Earthquake (GAE) occurred in Prince William Sound, Alaska, over 3000 km northwest of Monterey Bay. Also, the magnitude of these events differed greatly. Whereas the LPE had a surface-wave magnitude of 7.1, the GAE had a surface-wave magnitude of 8.3 on the Richter scale. Additionally, the tsunami associated with the LPE was generated inside the bay whereas the tsunami associated with the GAE was generated near the epicenter in the northern Gulf of Alaska, propagated as a tsunami across the Pacific basin and down the west coast of North America and was then transformed into a seiche upon entering Monterey Bay. In each case, these events were recorded at a tide gauge at  $36^{\circ}36.3'$ ,  $121^{\circ}53.3'$  in Monterey Harbor located in the inner bight of southern Monterey Bay. Fig. 1 shows Monterey Bay, the epicenter for the LPE, and certain aspects of the tsunamis and seiches associated with each event.



Figure 1. This figure shows Monterey Bay and depictions of the 1964 Great Alaskan Earthquake (GAE) tsunami (outside the bay) and the corresponding seiche (inside the bay), and the 1989 Loma Prieta Earthquake (LPE) tsunami and seiche (both inside the bay). The dotted line across the entrance of the bay represents the assumed location of the nodal line that corresponds to the node for transverse oscillations whose orientation is orthogonal to this line.

*Science of Tsunami Hazards, Vol. 28, No. 5, page 256 (2009)*

The natural oscillations of Monterey Bay, or seiche modes, have been a topic of interest for at least 40 years. Wilson, Hendrickson, and Kilmer (1965) examined the oscillating characteristics of Monterey Bay using a number of analytical and numerical techniques to estimate the expected periods of oscillation. Analytical and numerical methods were applied using various simple geometrical shapes to approximate the bay in order to extract its natural modes of oscillation. In applying these methods, a nodal line was assumed to exist across the mouth of the bay from the Monterey Peninsula to Santa Cruz (Fig. 1). In describing the oscillating characteristics of the bay, the mode of oscillation oriented in the North-South direction that spans the bay is referred to as longitudinal, and the mode of oscillation oriented in the East-West direction, where the existence of a nodal line is assumed, is referred to as transverse. The results of Wilson, Hendrickson, and Kilmer (1965) indicated that in addition to longitudinal and transverse modes of oscillation, many higher modes of oscillation can be excited that are primarily restricted to certain parts of the bay such as Monterey Harbor and the bight located in the Northeast quadrant of the bay east of Santa Cruz. They also found that the Monterey Submarine Canyon (MSC) has a profound effect on the natural oscillations that occur within the bay. The canyon serves to separate the bay into two semi-independent halves with only weak coupling between them. Finally, periods were predicted for the lowest modes in Monterey Bay. The periods for the first 6 modes were 44.2, 29.6, 28.2, 23.3, 21.6, and 20.4 minutes. Separate predictions were made for Monterey Harbor with periods ranging from 1-2 minutes, to 13.3 minutes. Observational studies have consistently shown natural periods of oscillation for the bay of approximately 55, 36, 27, and 21 minutes (e.g., Lynch, 1970; Breaker et al., 2008), where an oscillation with a period of 55 minutes corresponds to the first longitudinal mode, and an oscillation with a period of 36 minutes corresponds to the first transverse mode.

Thus, it is the primary purpose of this study to compare the sea level response of these events in terms of their frequency content as recorded by the tide gauges in Monterey Harbor. However, where the data permit and sufficient supporting information exists, we examine other aspects of these events as well.

## **2. MATERIALS AND METHODS**

### **Data Acquisition**

In this section we provide background information on tidal measurements in Monterey Harbor and the tide gauges that were used to acquire water level data during the 1964 Great Alaskan Earthquake (GAE) and the 1989 Loma Prieta Earthquake (LPE).

On May 23, 1960, Prof. Warren Thompson of the U. S. Naval Postgraduate School in Monterey, California, recorded sea level fluctuations in Monterey Harbor, associated with a magnitude 8.5 earthquake that occurred off Chile. He noted seiches, or water level oscillations, that caused the sea level to rise and fall as much as six feet over a 20-minute period. Thompson was not able to witness the tsunami's arrival, but was able to record water level oscillations in the bay that occurred as a result of the initial perturbation (Berkman and Symons, 1964). This led to an interest in recording tsunamis and other water level oscillations in southern Monterey Bay.

*Science of Tsunami Hazards, Vol. 28, No. 5, page 257 (2009)*

Thompson installed a Standard Tide Gauge in June 1963, which operated continuously until 1974.

The relatively simple Standard Gauge measures water levels directly through a system of pulleys and counterweights. It records water level on a strip chart or marigram, which is pulled forward by a clock mechanism. A float inside a protective well that extends at least a meter below the lowest anticipated tide level measures the water level. The standard opening at the bottom of the float well that is exposed to the ocean is reduced to 2 to 4 cm, to minimize interference by shorter wind waves. A pipe of the same inside diameter extends down 1.0 to 1.5 m below the orifice to reduce nonlinearities associated with higher frequency waves (Noye, 1974). The Standard Gauge records waves with periods from 30 to 60 seconds, to periods of several months (Bretschneider, 1983; Theberge, 2005). According to Cross (1967), the Standard Tide Gauge, similar to the one used by Thompson, “gives a good representation of tsunamis for periods larger than 5 minutes and wave heights of 2 feet (0.61 meters), or 15 minutes, for wave heights of 20 feet (6.1 meters).” We note that the periods and wave heights observed during this study did not exceed these limits.

In 1989, a Bubbler Tide Gauge was installed at Monterey according to the standards of NOAA’s National Ocean Service (NOS). This gauge served as a backup for other tide gauges that were in operation at Monterey at that time. This instrument, which produced an analog record, was used to record the Loma Prieta earthquake during October 1989. Rabinovich et al. (1999) found that the dynamic response of the Bubbler Gauge, installed to NOS standards, is highly dependent on period, but for periods of roughly 10 minutes or greater, the response was 95-98% of the observed changes in water level. Thus, the response of this gauge was marginally sufficient to reproduce the 9-10 minute period oscillations that we observed during this event. Since the Bubbler Gauge produced an analog record, it allowed us to digitize the data at sufficiently high resolution to insure that the highest frequencies, as recorded by the instrument, were retained.

### **Data Preparation**

For the GAE, paper records in the form of strip charts were obtained directly from the output of the tide gauge in Monterey Harbor for a period of approximately 72 hours starting several hours prior to the first arrival of this event. These strip charts were concatenated to produce a continuous 72-hour record. This record was next electronically scanned using a CONTEX FSC Model 5010, 36-inch Full Scale Color Scanner. A scanned record already existed for the tidal record at Monterey for the LPE. The scanned files were then imported into Photoshop where an image mask was applied and the original traces were isolated and assigned a color. Next, a program was written to import the traces into MATLAB and convert them into an RGB pixel image format. The image was then scanned to identify the trace in the MATLAB environment. Then information obtained from the original traces and from NOAA’s Tide Tables was added to calibrate the records. The final step in each case was to digitize the traces at a resolution of 39 seconds between samples along the abscissa, and to less than one centimeter, along the ordinate. The first 5 hours were digitized in this manner for the LPE, and the first 47 hours for the GAE.

## Singular Spectrum Analysis

Singular Spectrum Analysis (SSA) is based on a formal mathematical decomposition that consists of four steps. The first is the embedding step where a trajectory matrix is constructed from lagged versions of the original time series, second, a Singular Value Decomposition (SVD) of the matrix formed by the product of the trajectory matrix and its transpose, which corresponds to an eigenvalue problem that yields eigenvalues and eigenvectors, third, grouping, which involves splitting the matrices from the SVD into groups and summing the matrices within each group, and fourth, transforming the matrices into individual time series that can be summed to produce partial series, or if all of the individual series are summed, the original time series itself (e.g., Elsner and Tsonis, 1996; Golyandina et al., 2001). The method essentially decomposes the data into a set of independent modes where the user specifies the number of modes.

The embedding step can be accomplished by forming a trajectory matrix obtained from the time series,  $x_t$ , of length,  $N$ , where  $t=1, 2, \dots, N$ , as

$$\phi_{ij} = \frac{1}{N-L+1} \sum_{t=1}^{N-L+1} (x_{i+t-1} - \bar{x})(x_{j+t-1} - \bar{x}) \quad (1)$$

$L$  is the window length or embedding dimension and corresponds to the number of lagged vectors that are produced, each with dimension  $L$ ,  $1 \leq i \leq K$ , where  $K = N-L+1$ ,  $1 \leq j \leq L$ , and  $\Phi_{ij}$  is the trajectory matrix whose dimensions are  $K \times L$ . The mean value of the time series,  $\bar{x}$ , has been removed in each case prior to calculating  $\Phi_{ij}$ .

A lagged-covariance matrix,  $\tilde{M}$ , is then formed from the trajectory matrix,  $\Phi_{ij}$ , as follows

$$\tilde{M} = \frac{1}{K} \Phi^T \Phi \quad (2)$$

where  $\Phi^T$  is the transpose of  $\Phi$ . From the second step above, SVD is applied to  $\tilde{M}$  to extract the eigencomponents which include eigenvalues, eigenvectors, and the temporal principal components. When the square roots of the eigenvalues are plotted in descending order, we obtain the singular spectrum.

In conducting SSA, a suitable window length,  $L$ , must be chosen.  $L$  determines the number of lagged vectors that are used to form the trajectory matrix, and thus, the resolution of the decomposition. Values of  $L$  can vary from 2, to  $N-1$ , but usually vary between  $N/15$  and  $N/3$  (Vautard, 1995). According to Golyandina et al. (2001), the choice of  $L$  depends on the application but should be large enough so that each  $L$ -lagged vector includes an essential part of the behavior of the system. As a rule,  $L$  is usually varied over a range of values before a final value is chosen, but experience with the method and familiarity with the data are extremely helpful in making this choice.

### 3. RESULTS

#### **Loma Prieta Earthquake of 1989**

On October 18, 1989 at 0104 GMT, a surface-wave magnitude 7.1 earthquake occurred on the San Andreas fault in the Santa Cruz Mountains approximately 16 km northeast of Santa Cruz, California (McNutt, 1990). The corresponding seismic moment for this event was 6.9 on the moment magnitude scale. Consistent with this general description, a tsunami was generated that propagated across at least part of the bay, arriving at the tide gauge in Monterey Harbor approximately 20 minutes after the main event (Schwing et al., 1990). However, from the various reports that appeared following the Loma Prieta earthquake it is not exactly clear where and how the tsunami was generated. According to Schwing et al. (1990), and Gardner-Taggart and Barminski (1991), the tsunami may have been caused by vertical uplift from the initial shock wave at the coast near Santa Cruz. However, subsequent observations in Monterey Submarine Canyon indicate that this earthquake produced offshore landslides along the walls of the canyon (Gardner-Taggart and Barminski, 1991), slumping along the south wall of the canyon (Greene et al., 1991), and turbidity currents (Garfield et al., 1994), processes that each could have generated a tsunami. Ma et al. (1990) produced a synthetic tsunami for the bay based on the seismic characteristics of the earthquake and concluded that large-scale slumping near Moss Landing could have generated a tsunami similar to that observed at Monterey. It is possible, and perhaps likely, that more than one process contributed to the observed sea level response at Monterey. The height of a tsunami can be roughly estimated near the source of generation according to

$$\text{Log}_{10}H = 0.75M - 5.07 \quad (3)$$

where H is the wave height in meters and M is the Richter or surface-wave magnitude (e.g., Camfield, 1980). However, this empirical relationship does not completely take into account the characteristics of the generating mechanism or the coastline. Also, we prefer to use the moment magnitude instead of the surface-wave magnitude because of its improved physical basis including the fact that it does not tend to saturate at higher magnitudes (e.g., Bryant, 2001). However, as we shall see in the following section, using the moment magnitude instead of the surface-wave magnitude does not always produce better results. Using (3), with a value for M of 6.9, we obtain a value of 1.3 meters for the LPE. The period of a tsunami can be estimated according to

$$\text{Log}_{10}T = 0.625M - 3.31 \quad (4)$$

(Wilson and Torum, 1968), where T is the period in minutes and M is the magnitude. In this case, we obtain a period of 10.1 minutes. Estimates of the amplitude and period of this event provide a basis for comparison with the observed sea level response at Monterey.

In the top panel of Fig. 2 (Fig. 2a), the tide gauge record for the three-day period from 17-20 October 1989 is shown. In the lower panel (Fig. 2b) we have extracted a 5-hour segment of this record for closer inspection. The primary response to this event appears to have taken

place during the first 15 hours or so after  $t_0$  (the first arrival of the event), although weaker indications could be observed in the record for up to 3 days. Following the main event, the two largest aftershocks were of magnitude 5.2 and 5.0 on the Richter scale (McNutt, 1990), and so were not sufficient to generate additional tsunamis (e.g., Wilson et al., 1962). According to Murty et al. (2006) and Murty et al. (2008), the influence of tsunamis can last for several days due to arrivals from the same event that have taken multiple paths through reflections, energy trapping, and secondary undulations.

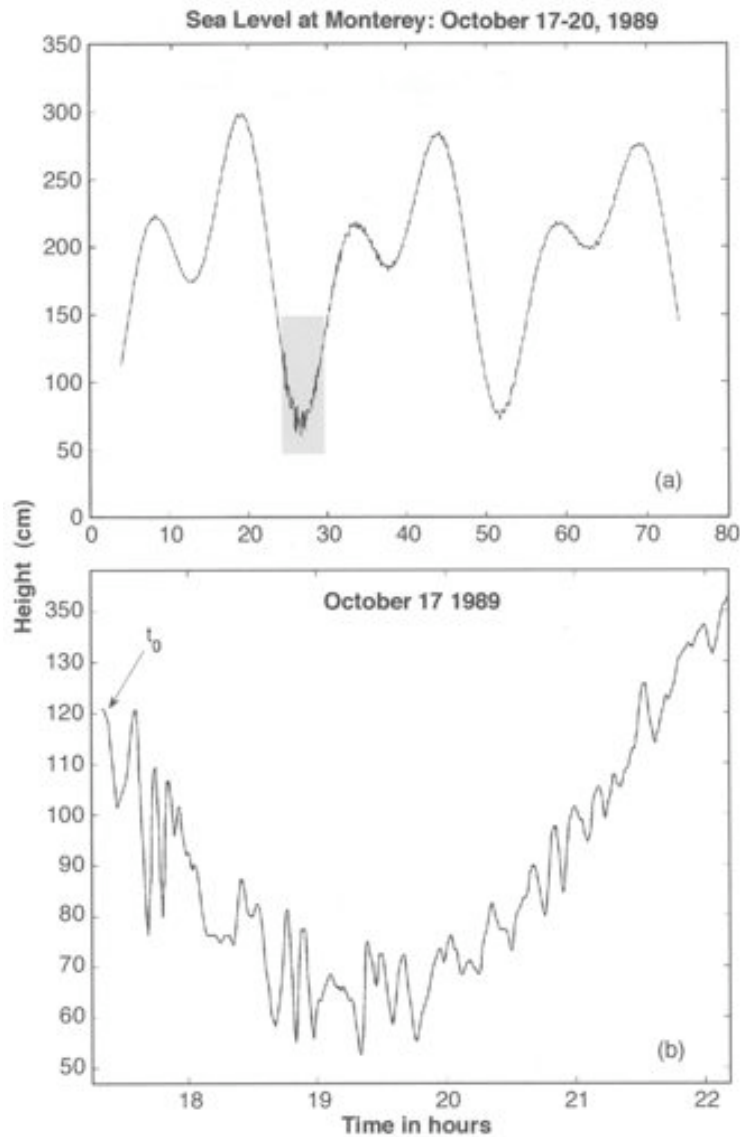


Figure 2. The top panel, (a), shows a segment of the tidal record at Monterey during the period of the LPE from 17 to 20 October 1989. The area shaded in gray corresponds to the first five hours of this event. The lower panel, (b), shows the first five hours in greater detail where  $t_0$  indicates the first arrival of this event.

The apparent maximum range of variability during the period shown in Fig. 2b is of the order of 45 cm. However, due to the response characteristics of the tide gauge employed and the subsequent data processing, this record may underestimate the true amplitude of the signal, significantly. If our estimate of the initial wave height (1.3 meters) is realistic, then a maximum observed range of 45 cm is smaller than the predicted wave height by almost a factor of 3.

Singular Spectrum Analysis (SSA) has been applied to the record shown in Fig. 3b in order to extract the primary frequencies contained therein. The eigenvalues in Fig. 3a show how the variance is partitioned by mode. A window length,  $L$ , of 300 (3.25 hours) was chosen.

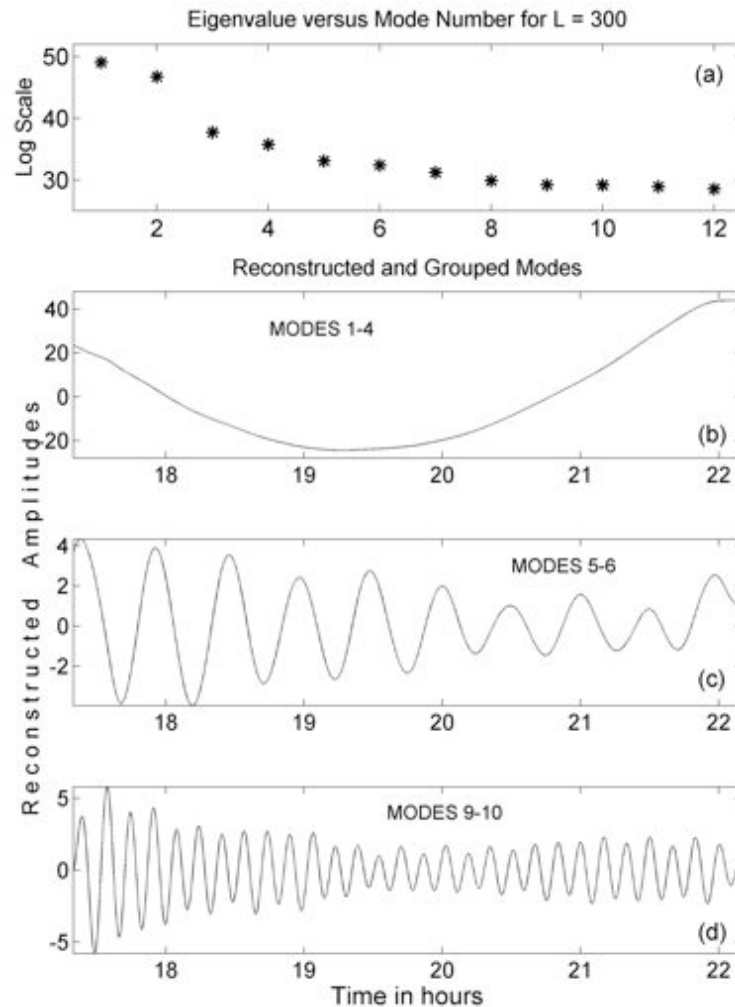


Figure 3. The top panel, (a), shows the distribution of eigenvalues for the first 12 modes of the singular spectrum analysis for the record shown in Fig. 2b, for a window length of 300 (3.25 hours). The scale on the vertical axis is logarithmic. The second panel, (b), shows the first four reconstructed modes which correspond to the astronomical tide. The third panel, (c), shows reconstructed modes 5 and 6, which reveal an oscillation with a period of 31-32 minutes, and the bottom panel, (d), shows reconstructed modes 9 and 10, which reveal an oscillation with a period of 9-10 minutes.



The first 4 modes account for 88.6%, and the first 10 modes, 93.6%, of the total variance. When the first four modes are reconstructed and grouped, they closely approximate the underlying tidal signal (Fig. 3b). When modes 5 and 6 are combined (Fig. 3c), they correspond to an oscillation with a period of 31-32 minutes. Again, this period is not fixed, but varies slightly. A period of 31-32 approaches the expected period of transverse oscillation for the bay. The transverse mode as described by Wilson et al. (1965) has a nodal line across the entrance of the bay and an antinode at Moss Landing (Fig. 1). The expected period is approximately 36 minutes and has been observed on a number of occasions, and, again, as we shall see, after we examine the GAE. Modes 9 and 10, taken together (Fig. 3d), reproduce an oscillation with a period of 9-10 minutes, consistent with the findings of Schwing et al. (1990). This oscillation does not represent a pure tone, but, rather, one whose period varies slightly, i.e., it is frequency modulated. The period is close to the predicted period of the tsunami itself which was 10.1 minutes. However, it is likely that the tsunami associated with the LPE was at least partially influenced by the boundaries of the bay when it arrived at Monterey Harbor and so its frequency content may have been altered as it propagated south and began to take on the characteristics of a seiche. Finally, a period of 9-10 minutes falls well within the range of seiche periods for Monterey Harbor as predicted by Wilson et al. (1965).

### **The Great Alaskan Earthquake of 1964**

On March 28, 1964 at 03:36 GMT, a shallow earthquake of surface-wave magnitude 8.3 and a moment magnitude of 9.2 occurred at 61.0°N, 147.8°W in Prince William Sound, in south-central Alaska (Page, 1968). Uplifting caused vertical displacements as large as 16 m on the sea floor in the vicinity of the epicenter (Malloy, 1964). According to Plafker and Mayo (1965), submarine uplift of the continental shelf within Prince William Sound and considerably beyond, generated a train of long-period large-amplitude seismic sea waves, or tsunamis, that were recorded at tide gauges throughout the Pacific basin. The tsunami that was generated by this earthquake propagated across the Pacific basin and south along the west coast of North America reaching the latitude of Monterey Bay at approximately 08:18 GMT on March 28, 1964. During the first day following the main event there were 11 aftershocks of surface-wave magnitude 6.0, or greater (Page, 1968), but none large enough to generate a second tsunami.

Cylindrically symmetrical dispersive waves decay approximately according to  $1/r$ , where  $r$  is the distance from the epicenter, and the effects of bottom depth are not taken into account. However, when the tsunami approaches the coast the effects of bottom depth must be taken into account, and both refraction and dispersion may become important. Thus, without the help of a numerical model that contains the governing physics and the appropriate initial and boundary conditions, it is not a simple matter to estimate the height of the tsunami when it reached Monterey Bay. Since the period remains essentially constant we can estimate this parameter, and using equation (4) with a magnitude of 8.3, we obtain a value of 75.4 minutes. This value is very close (a difference of less than 1 minute) to the period of positive surge observed at Wake Island following the GAE (Van Dorn, 1964). We note that using a moment magnitude of 9.2 in this case predicts a period of almost 4.6 hours which is far greater than the period that was observed for this event.

Fig. 4a shows a digitized version of the strip chart that was originally recorded from the tide gauge in Monterey Harbor for the two-day period (actually, 47 hours) following the first arrival of this event at  $t_0$ . In Fig. 4b, we have extracted a 5-hour portion of the record. The peak-to-trough range of the oscillations associated with this event approach, or even exceed, 100 cm, rivaling the amplitude of the semidiurnal tide itself. Over the first two days, the amplitudes of the oscillations associated with this event decrease by roughly an order-of-magnitude. However, oscillatory behavior could be detected for at least four days following the main event, due to multipath effects, which spread the arrival pattern over time.

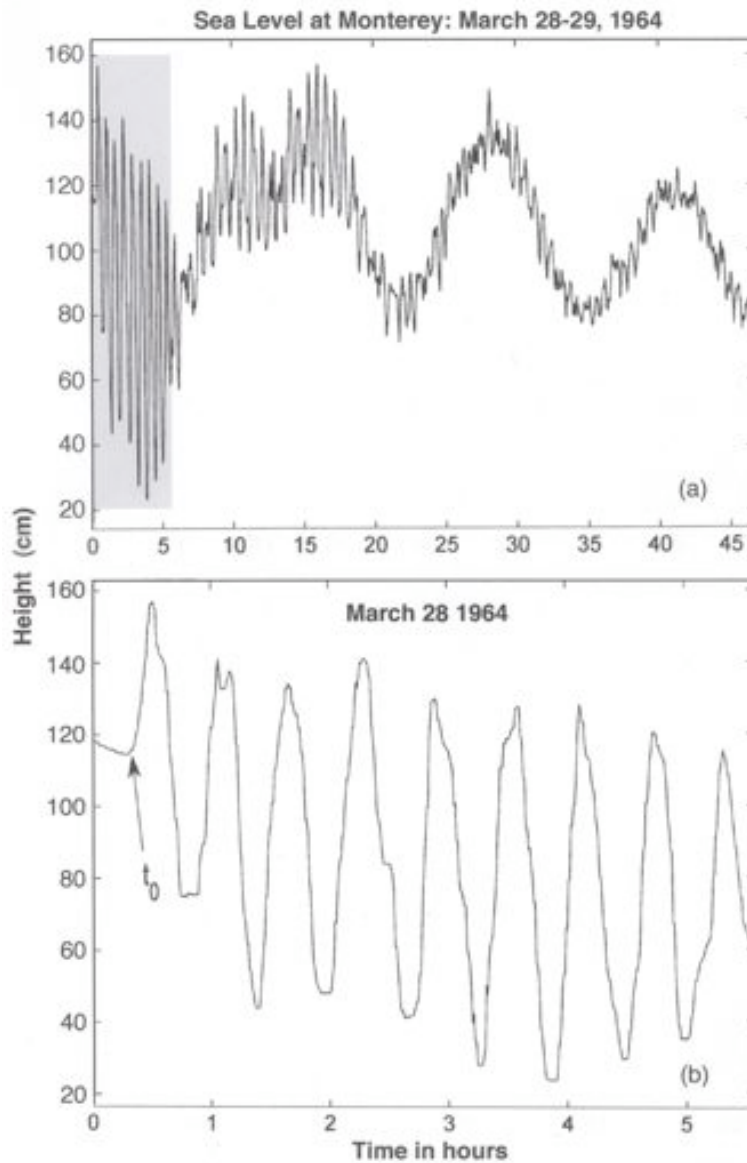


Figure 4. The top panel, (a), shows a segment of the tidal record at Monterey during the period of the GAE from 28 to 29 March 1964. The area shaded in gray corresponds to the first five hours of this event. The lower panel, (b), shows the first five hours in greater detail where  $t_0$ , again, indicates the first arrival of this event.

An examination of the record in Fig. 4a shows that two bursts of 6 or 7 oscillations followed within 2-3 hours of the initial burst, which consists of 10 oscillations. After the first 20 hours, the oscillations continue but are no longer burst-like. They are more continuous in nature with amplitudes that gradually decrease with time. This trend continues out to four days at which time the oscillations were barely detectable (not shown). The second two bursts that follow the initial burst suggest that they could be due to reflections that occurred relatively close to the epicenter because of their similarity to the initial burst. Because there are no obvious reflecting boundaries outside Monterey Bay for great distances it is unclear how reflections could play a significant role in contributing to these secondary oscillations unless they occurred much closer to the epicenter. The initial disturbance could have been reflected from bathymetric features along the Aleutian Chain as it spread southward from the epicenter. However, without detailed calculations that take into account the possible propagation paths that could have produced arrival times matching those in the record, we cannot answer this question. Thus, we also consider energy trapping and secondary undulations as processes that may have contributed to the extended oscillations. Energy trapping can take the form of continental shelf waves that are trapped over the continental margin by the sloping bottom and are strongly influenced by the earth's rotation. However, because these waves are generated and propagate along the open coast it is unlikely that they are responsible for the extended oscillations observed in the tide gauge record at Monterey. Energy trapping can also generate infragravity waves called edge waves, which appear to have been previously observed in Monterey Bay (MacMahan et al., 2004a; MacMahan et al., 2004b). Yanuma and Tsuji (1998) showed that using a shelf slope of 1/1000 and a shelf width of 1 km, a period of approximately 27 minutes is predicted for the first standing edge wave mode. In the shallow shelf regions of Monterey Bay, away from MSC, edge waves with periods of the same order are predicted.

According to Kowalik and Murty (1993), secondary undulations are oscillations whose periods correspond to the normal modes of the bay and can be excited by a number of different sources, including tsunamis. These secondary undulations can be classified rather generally as one of three types, A, B, or C, depending on the geometry of the bay (Nakano, 1932). In type A, the secondary undulations appear as coherent wave trains with approximately the same waveform. In type B, they are not as regular and coherent as in type A, but are not completely irregular. In type C, they are essentially irregular in form. The type of secondary undulations can be roughly determined by plotting the depth of the bay versus  $10S/b^2$ , where  $S$  corresponds to the surface area of the bay and  $b$  is its breadth. For Monterey Bay, with a surface area,  $S$ , of roughly 800 km<sup>2</sup>, a breadth of approximately 20 km, and an average depth of 100m, we find that secondary undulations fall into category B, where they are not as regular and coherent as in type A, but are not completely irregular. On a qualitative basis, we find this result is generally consistent with the oscillatory patterns exhibited in the record. In summary, although the pair of secondary bursts between hours 8 and 18 in Fig. 4a may be due to reflections, we are not able to identify any reflecting boundary near Monterey Bay that may have been responsible. Both edge waves and secondary undulations inside the bay provide reasonable explanations for the observed pattern of oscillations that lasted for up to 4 days following the initial burst.

We have applied SSA to this record as well. Fig. 5a shows the first 10 eigenvalues, which account for over 90% of the total variance. A window length of 1000 or 10.8 hours was used,

which is about 23% of the record length. When the first three modes are reconstructed and grouped (Fig. 5b), they approximately represent the predicted semidiurnal tide, at least for the last two cycles.

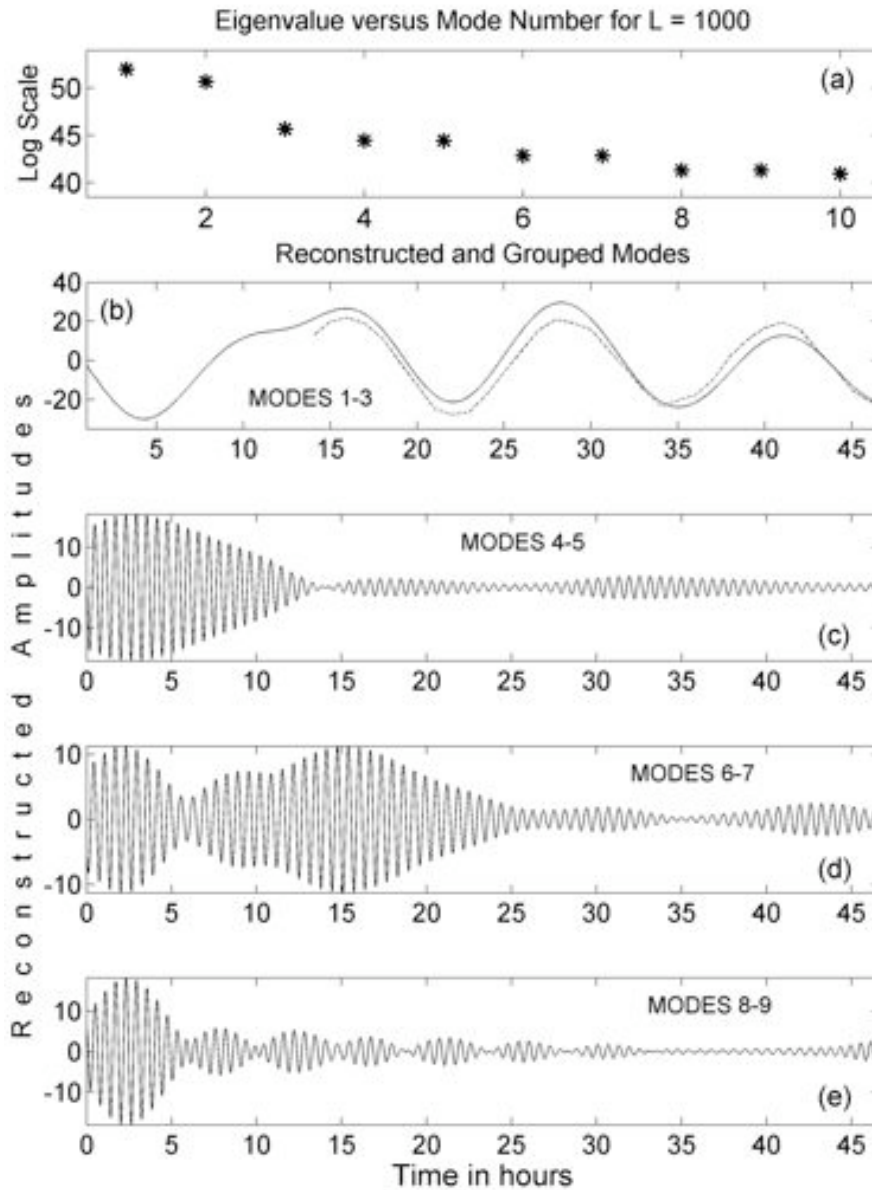


Figure 5. The top panel, (a), shows the distribution of eigenvalues for the first 10 modes of the singular spectrum analysis for the record shown in Fig. 4, for a window length of 1000 (10.8 hours). The second panel, (b), shows the first three reconstructed modes, which correspond to the astronomical tide. The dashed line shows the corresponding semidiurnal tide from the NOAA Tide Tables for 1964. The third panel, (c), shows reconstructed modes 4 and 5, the fourth panel, (d), reconstructed modes 6 and 7, and the fifth or bottom panel, (e), reconstructed modes 8 and 9. The period in each case is approximately 37 minutes.

During the first 10-15 hours, nonlinear interaction between the tidal signal and the tsunami-driven seiche may have occurred, leading to distortion in the observed waveform. When modes 4 and 5, 6 and 7, and 8 and 9 are reconstructed and grouped, they each have a period of approximately 37 minutes,  $\pm 0.5$  minutes. Each grouping appears to represent a different aspect of the same oscillation, most likely, separate arrivals that occurred during the period of observation. An observed oscillation with a period of approximately 37 minutes is in close agreement with the past observations of Lynch (1970) and Breaker et al. (2008). A period of 37 minutes corresponds closely to the expected transverse mode of oscillation for the bay that assumes a nodal line across the entrance from the Monterey Peninsula to Santa Cruz (Fig. 1). This mode of oscillation is consistent with a tidal wave that enters the bay from the west. As the wave conforms to the bay's dimensions, it is transformed into a seiche whose period has often been observed, and at least approximately predicted by Wilson et al. (1965). We also note that a period of 37 minutes corresponds to a frequency that is approximately twice the frequency associated with the period of the 1964 tsunami, which was about 75 minutes. This raises the question of resonance between the incoming tsunami and the corresponding seiche it produced. If we consider the case of harbor resonance, as described by LeBlond and Mysak (1988), where the wave motion is excited by forcing at the entrance, the response may be expressed as the ratio of the maximum amplitude inside the harbor to the amplitude at the entrance. The simplest case of a resonant response occurs for quarter-wave resonance. In this case the only processes that limit the amplitude inside the harbor are dissipative in nature. In harbors where this happens, the entrance corresponds to a nodal line and the antinode occurs at a distance of one-quarter wavelength inside the harbor (Fig. 1). This appears to be the same situation that has occurred in Monterey Bay with respect to the GAE. And since the resonant frequency of the bay for the transverse mode is almost an integer multiple of the forcing frequency, the opportunity for resonant interaction to occur may have been enhanced. Finally, although the groupings for modes 4 and 5, 6 and 7, and 8 and 9 are independent, each represents the same frequency, a result that we have not previously encountered in the application of SSA.

#### 4. CONCLUSIONS

Singular Spectrum Analysis (SSA) was particularly effective in extracting the primary frequencies associated with each event, consistent with the findings and recommendations of Golyandina et al. (2001), and Ghil et al. (2002). It is not clear how or exactly where the tsunami associated with the 1989 Loma Prieta Earthquake (LPE) was generated in Monterey Bay, although these questions have been discussed in the literature. It may have been initiated at the north end of the bay near Santa Cruz, along the south wall of Monterey Submarine Canyon, or further up the canyon near Moss Landing. It is most likely that the tsunami generated by the LPE began to take on the characteristics of a seiche by the time it reached the tide gauge in Monterey Harbor. Our results indicate that the LPE was responsible for generating one mode of oscillation with a period of 9-10 minutes, generally consistent with the predicted periods of oscillation for Monterey Harbor, and a second oscillation with a period of 31-32 minutes that most likely corresponds to a bay-wide oscillation.

*Science of Tsunami Hazards, Vol. 28, No. 5, page 267 (2009)*

The initial peak-to-trough amplitude of the sea level response to the GAE was close to 100 cm and thus of the same order as the amplitude of the semidiurnal tide itself. Two bursts of 6-7 oscillations followed within 2 to 3 hours after the initial burst of 10 oscillations and may have been due to reflections of the main event and thus taken a slightly longer path on their way across the Pacific. We conclude that edge waves and secondary undulations may have also contributed to the oscillatory behavior observed in the sea level record out to a period of almost 4 days. SSA revealed oscillations with a period of approximately 37 minutes, which corresponds to the transverse mode of oscillation that has previously been observed. Although different arrivals were included in the SSA decomposition, only a single frequency with a period of ~37 minutes was found, consistent with a strongly resonant response. This mode of oscillation is consistent with a tidal wave that entered the bay from the west where a nodal line extends across the entrance from the Monterey Peninsula to Santa Cruz. We conclude that the tsunami produced quarter-wave resonance within the bay consistent with the observed seiche-like response in sea level.

The sea level responses to the LPE and the GAE were entirely different, not only because of the large difference in the magnitudes of these events, but also because the driving force in one case occurred inside the bay (LPE), and in the second, outside the bay (GAE). As a result, different modes of oscillation were excited.

## **5. ACKNOWLEDGMENTS**

Charlie Endris from Moss Landing Marine Laboratories is thanked for helping us to scan the original strip chart record for the Great Alaskan Earthquake of 1964.

## **6. REFERENCES**

- Berkman, S.C. and J.M. Symons, (1964). The tsunami of May 22, 1960 as recorded at tide stations. U.S. Department of Commerce, Coast and Geodetic Survey, Washington 25, D.C., 69pp.
- Bretschneider, D., (1983). Sea level variations at Monterey, CA, U.S. Dept. Commer. NOAA Tech. Rep. NMFS SSRF-761, 50 pp.
- Bryant, E., (2001). TSUNAMI: The Underrated Hazard. Cambridge University Press, Cambridge, UK.
- Camfield, F.E., (1980). Tsunami Engineering. Special Report No. 6. U.S. Army, Corps of Engineers, Coastal Engineering Research Center, Fort Belvoir, VA, 222 pp.
- Cross, R. H., (1967). Frequency response of tide gages. University of California, Berkeley, Hydraulic Engineering Laboratory, Technical Reports HEL, 16 - 2,3,4.

*Science of Tsunami Hazards, Vol. 28, No. 5, page 268 (2009)*

- Elsner, J.B. and A.A. Tsonis, (1996). Singular Spectrum Analysis: A New Tool in Time Series Analysis. Plenum Press, New York and London.
- Gardner-Taggart, J.M. and R.F. Barminski, (1991). Short period wave generation in Moss Landing harbor caused by offshore landslides induced by the Loma Prieta earthquake. Geophysical Research Letters, 18, 1277-1280.
- Garfield, N., T.A. Rago, K.J. Schnebele, and C.A. Collins, (1994). Evidence of a turbidity current in Monterey Submarine Canyon associated with the 1989 Loma Prieta earthquake. Continental Shelf Research, 14, 673 - 686.
- Ghil, M., M.R. M.D. Allen, K. Dettinger, D. Kondrashow, M.E. Mann, A.W. Robertson, A. Saunders, Y. Tian, F. Varadi, and P. Yiou, (2002). Advanced spectral methods for climatic time series. Reviews of Geophysics, 40, 1003, 3-1 – 3-41.
- Gohres, H., (1964). Tidal Marigrams, San Diego Historical Society Quarterly. October 1964, 10 (4), <http://www.sandiegohistory.org/journal/64october/marigram.htm>.
- Golyandina, N., V. Nekrutkin and A. Zhigljavsky, (2001). Analysis of Time Series Structure: SSA and Related Techniques. Monographs on Statistics and Applied Probability 90. Chapman & Hall/CRC, Boca Raton.
- Greene, H.G., J. Gardner-Taggart, M.T. Ledbetter, R. Barminski, T.E. Chase, K.R. Hicks and C. Baxter, (1991). Offshore and onshore liquefaction at Moss Landing spit, central California - result of the October 17, 1989, Loma Prieta earthquake. Geology, 19, 945 - 949.
- Kowalik, Z., and T.S. Murty, (1993). Numerical Modeling of Ocean Dynamics. World Scientific, Singapore.
- LeBlond, P.H. and L.A. Mysak, (1978). Waves in the Ocean. Elsevier Oceanography Series 20. Elsevier Scientific Publishing Company, Amsterdam.
- Ma, K., K. Sataki and H. Kanamori, (1990). Tsunami of the 1989 Loma Prieta earthquake (abstract). EOS Transactions AGU, 71, pp. 1460.
- MacMahan, J.H., J.H. Reniers, E.B. Thornton and T.P. Stanton, (2004a). Infragravity rip current pulsations. Journal of Geophysical Research, 109, C01033, doi: 10.1029/2003JC002068.
- MacMahan, J.H., J.H. Reniers, E.B. Thornton and T.P. Stanton, (2004b). Surf zone eddies coupled with rip current morphology. Journal of Geophysical Research, 109, C07004, doi: 10.1029/2003JC002083.

- Malloy, R.J., (1964). Crustal uplift southwest of Montague Island, Alaska. *Science*, 146, 1048-1049.
- McNutt, S., (1990). Loma Prieta earthquake, October 17, 1989. *California Geology*, 43, 3 - 7.
- Murty, T.S., (1977). Seismic Sea Waves: Tsunamis. *Bulletin of the Fisheries Research Board of Canada*, Bulletin 198, Ottawa, Canada.
- Murty, T.S., N.P. Kurian, and M. Baba, (2006). Trans-oceanic reflection of tsunamis: the Kerala example. *Disaster & Development*, 1, 65 - 76.
- Murty, T.S., N.P. Kurian, and M. Baba, (2008). Roles of reflection, energy, trapping and secondary undulations in the tsunami on Kerala coast. *International Journal of Ecology & Development*, 10, 100-114.
- Nakano, M., (1932). Preliminary note on the accumulation and dissipation of the energy of secondary undulations in a bay. *Proc. Phys. Math. Soc. Japan*, SER 3, 44-56.
- Noye, B.J., (1974). Tide-well systems II: the frequency response of linear tide-well system. *Journal of Marine Research*, 32, 155 -181.
- Page, R., (1968). Aftershocks and microaftershocks of the Great Alaska Earthquake of 1964. *Bulletin of the Seismological Society of America*, 58, 1131-1168.
- Plafker, G. and L.R. Mayo, (1965). Tectonic deformation, subaqueous slides and destructive waves associated with the Alaskan March 27, 1964 earthquake. *Open File Report, U.S. Geological Survey, Menlo Park, CA*, 19 pp.
- Rabinovich, A.B., R.E.Thomson, E.A. Kulikov, B.D.Bornhold and I. V. Fine, (1999). The landslide-generated tsunami of November 3, 1994 in Skagway Harbor, Alaska: A case study. *Geophysical Research Letters*, 26, 3009 -3012.
- Schwing, F.B., J.G. Norton and C.H. Pilskaln, (1990). Earthquake and bay response of Monterey Bay to the Loma Prieta earthquake. *EOS Transactions of the American Geophysical Union*, 71, 250-251, 262.
- Theberge, A.E., (2005). 150 years of tides on the western coast, the longest series of tidal observations in the Americas. *Center for Operational Oceanographic Products and Services, National Ocean Service, NOAA, DOC, Washington, D.C.*, 15 pp. [http://co-ops.nos.noaa.gov/publications/150\\_years\\_of\\_tides.pdf](http://co-ops.nos.noaa.gov/publications/150_years_of_tides.pdf)
- Van Dorn, W.G., (1964). Source mechanism of the tsunami of March 28, 1964 in Alaska. *Proceedings of the Ninth Conference on Coastal Engineering, American Society of Civil Engineers*, Chap. 10, 166-190.



- Vautard, R., (1995). Patterns in time: SSA and MSSA. In: von Storch, H., Navarra, A. (Eds.), Analysis of Climate Variability: Applications of Statistical Techniques. Springer-Verlag, Berlin, pp. 259-279.
- Wilson, B.W., L.M. Webb and J.A. Hendrickson, (1962). The nature of tsunamis: their generation, and dispersion in water of finite depth. Technical Report no. SN 57-2, National Engineering Science Company, 150 pp.
- Wilson, B.W. and A. Torum, (1968). The tsunami of the Alaskan earthquake, 1964: engineering evaluation. TM-25, U.S. Army Coastal Engineering Research Center, Washington, D.C.
- Yanuma, T. and Y. Tsuji, (1998). Observations of edge waves trapped on the continental shelf in the vicinity of Makurazaki Harbour, Kyushu, Japan. Jour. Oceanog., 54, 9-18.

